# Preparative and structural studies on iron(II)–thiolate cyanocarbonyls: Relevance to the [NiFe]/[Fe]-hydrogenases

**ARTICLE** *in* DALTON TRANSACTIONS · FEBRUARY 2004

Impact Factor: 4.2 · DOI: 10.1039/b311059a · Source: PubMed

FULL PAPER

Dalton
www.rsc.org/dalton

# Preparative and structural studies on iron(II)–thiolate cyanocarbonyls: relevance to the [NiFe]/[Fe]-hydrogenases

**Chien-Hong Chen,[a] Yung-Su Chang,[b] Chien-Yeh Yang,[b] Tai-Nan Chen,[a] Chien-Ming Lee[a] and Wen-Feng Liaw*[a]**

[a] *Department of Chemistry, National Tsing Hua University, Hsinchu 30043, Taiwan*

[b] *Department of Chemistry, National Changhua University of Education, Changhua, Taiwan. E-mail: wfliaw@mx.nthu.edu.tw*

***Received 10th September 2003, Accepted 5th November 2003***
***First published as an Advance Article on the web 24th November 2003***

A number of thermally stable iron(II)–thiolate cyanocarbonyl complexes, *cis*,*cis*-$[Fe(CN)_2(CO)_2(CS_3\text{-}S,S)]^{2-}$ (**1**), *mer*-$[Fe(CO)_2(CN)_3(NCCH_3)]^-$ (**2**) *mer*-$[Fe(CO)_3(CN)(CS_3\text{-}S,S)]^-$ (**3**), *cis*-$[Fe(CO)_2(CN)(S(CH_2)_2S(CH_2)_2S\text{-}S,S,S)]^-$ (**4**), $[Fe(CO)_2(CN)_3Br]^{2-}$ (**5**), *mer*-$[Fe(CO)_2(CN)_3(m\text{-}SC_6H_4Br)]^{2-}$ (**6**) and *mer*-$[Fe(CO)_2(CN)_3(SPh)]^{2-}$ (**7**) were isolated and characterized by IR and X-ray diffraction analysis. The extrusion of one strong σ-donor $CN^-$ ligand instead of CO from the iron(II) center of the thermally stable complexes $[Fe^{II}(CO)_2(CN)_3Br]^{2-}$ (**5**) containing less electron-donating bromide reflects the electron-rich character of the mononuclear $[Fe^{II}(CN)_2(CO)_2(CS_3\text{-}S,S)]^{2-}$ (**1**) when ligated by by the bidentate thiolate, and the combination of one cyanide, two carbonyls and a tridentate thiolate provides the stable complex **4** as a result of the reaction of complex **5** and chelating ligand $[S(CH_2)_2S(CH_2)_2S]^{2-}$. The preference of the sixth ligand coordinated to the unsaturated $[Fe^{II}(CO)(CN)_2(CS_3\text{-}S,S)]^{2-}$ Fe(II) center, the iron-site architecture of the bimetallic Ni–Fe active-site of [NiFe] hydrogenases, is a strong π-acceptor CO group. Scrutiny of the coordination chemistry of iron(II)–thiolate cyanocarbonyl species $[Fe^{II}(CO)_x(CN)_y(SR)_z]^{n-}$ reveals that certain combinations of thiolate, cyanide and carbonyl ligands ($3 \le y + z \le 4$) bound to Fe(II) are stable and this could point the way to understand the reasons for Nature's choice of combinations of these ligands in hydrogenases.

## Introduction

During the past few years, iron–thiolate complexes with mixed $CN^-$ and CO ligands have drawn the attention of bioinorganic/bioorganometallic chemists in their pursuit of synthesizing penta-/hexa-coordinate iron(II)–thiolate cyanocarbonyl complexes,[1–5] since the active-site $[(S_{cys})_2Ni(\mu\text{-}S_{cys})_2(\mu\text{-}X)Fe(CO)(CN)_2]$ (X = O, OH) of [NiFe]-hydrogenases isolated from *Desulfovibrio gigas* has been established as a pyramidal $[Fe(CN)_2(CO)]$ unit with the opposite face coordinated to two cysteines bridged to a nickel.[6,7] The X bridge is assumed to be absent in the reduced active state of the enzyme.[6,7] EPR studies indicated the nickel site serves as a redox center and the iron site remains as Fe(II) in all spectrally defined redox states (Ni–A, Ni–B, Ni–SI, Ni–C, Ni–R, Ni–L states) of the enzyme.[8] In [Fe]-hydrogenases, the X-ray crystal structure of [Fe]-hydrogenases from *Clostridium pasteurianum* (CpHase)/*Desulfovibrio desulfuricans* (DdHase) indicated that the active-site cluster consists of a [4Fe–4S] cubane subcluster covalently bridged by a cysteine to a dinuclear iron–thiolate–cyanocarbonyl subcluster with iron atoms coordinated by CO and $CN^-$ groups.[9,10]

The iron sites of both families of hydrogenases feature $CN^-$ ligands in addition to cysteines and CO. A deep understanding of the relative affinities of Fe(II) for cyanides *vs*. thiolates is relevant to the entire theme of metallo-hydrogenases.[2–5] Therefore, a varying number of these donor groups can be assembled in a designed complex to tune the redox and catalytic properties of the iron center. In addition, structural models as $[Fe^{II}(CO)_x(CN)_y(SR)_z]^{n-}$ may be appreciated as possibilities for intermediates in the biosynthesis of [NiFe]-hydrogenase active-sites, although the assembly of Fe–CN–CO building blocks and nickel tetracysteines have been addressed recently by Casalot and Rousset in the "*Maturation of the [NiFe] Hydrogenases*".[11]

Recently, a few mononuclear iron–thiolate cyanocarbonyl compounds $([CpFe(CN)_2(CO)]^-$ (Cp = $\eta^5$-cyclopentadienyl), $[Fe(CN)_2(CO)(S_2C_6H_4\text{-}S,S)]^{2-}$, $[(PS3)Fe(CN)(CO)]^{2-}$ ($PS3H_3$ = tris(2-phenylthiol)phosphine), and $[(S_3)Fe(CN)_2(CO)]^{2-}$ ($S_3$ = bis(2-mercaptophenyl) sulfide(2−))) have been reported by Darensbourg *et al.*,[1] Rauchfuss *et al.*,[2] Koch and co-workers[3] and Sellmann *et al.*,[4] respectively. We have also shown that complexes $[Fe(CO)_4(CN)]^-$ and $[Fe(CO)_3(CN)_2Br]^-$ serve as the useful precursors to yield Fe–CN–CO–SR species, $[Fe(CO)_2(CN)(SNHC_6H_4\text{-}N,S)]^-$, $[Fe(CO)(CN)(SC_5H_3N)_2]^-$, $[Fe(CN)_2(CO)_2(S_2CR\text{-}S,S)]^-$, and $[Fe(CN)_2(CO)(S_2CR\text{-}S,S)]^-$ (R = OEt, $NEt_2$), respectively.[5] We undertook the present exploratory project aimed at expanding the range of Fe–CO–CN–SR derivatives which may provide valuable insight related to the structure, spectroscopic properties and reactivity of iron-containing hydrogenases. Herein, we report the synthesis and characterization of a number of the thermally stable iron(II)–thiolate cyanocarbonyl complexes, *cis*,*cis*-$[Fe(CO)_2(CN)_2(CS_3\text{-}S,S)]^{2-}$ (**1**), *mer*-$[Fe(CO)_2(CN)_3(NCCH_3)]^-$ (**2**), *mer*-$[Fe(CO)_3(CN)(CS_3\text{-}S,S)]^-$ (**3**), *cis*-$[Fe(CO)_2(CN)(S(CH_2)_2S(CH_2)_2S\text{-}S,S,S)]^-$ (**4**), $[Fe(CO)_2(CN)_3Br]^{2-}$ (**5**), *mer*-$[Fe(CO)_2(CN)_3(m\text{-}SC_6H_4Br)]^{2-}$ (**6**), and *mer*-$[Fe(CO)_2(CN)_3(SPh)]^{2-}$ (**7**). This study demonstrates that a certain total number of thiolate and cyanide ligands ligated to the Fe(II) center provides significant stabilization to the iron(II)–thiolate cyanocarbonyl species $[Fe^{II}(CO)_x(CN)_y(SR)_z]^{n-}$.

## Results and discussion

Reaction of $K_2CS_3$ and $[Fe(CO)_3(CN)_2Br]^-$ in 1 : 1 stoichiometry proceeds in $CH_3CN$ under $N_2$ at ambient temperature to form *cis*,*cis*-$[Fe(CN)_2(CO)_2(CS_3\text{-}S,S)]^{2-}$ (**1**) identified by IR and X-ray diffraction analysis (Scheme 1(a), (b)). The dianionic complex **1** exhibits a two-band pattern in the $\nu_{CO}$ region (2016s, 1960s $cm^{-1}$ ($CH_3CN$) supporting a *cis* position of two CO groups, and the two weak absorption bands 2111w, 2102w $cm^{-1}$ assigned to the cyanide stretching frequencies support a *cis* position of two $CN^-$ ligands. Exposure of complex **1** to $^{13}CO$ gives rise to a two-band pattern (1970s, 1915s $cm^{-1}$) of IR $\nu_{CO}$ bands at 25 °C overnight to afford $^{13}C$-enriched derivative *cis*,*cis*-$[Fe(CN)_2(^{13}CO)_2(CS_3\text{-}S,S)]^{2-}$. Reappearance of the 2016s, 1960s $cm^{-1}$ bands on removal of the $^{13}CO$ and replacement with $^{12}CO$ atmosphere demonstrated reversibility of CO ligand lability of complex **1**. In contrast, under similar reaction condition, complex *mer*-$[Fe(CO)_2(CN)_3(NCCH_3)]^-$ (**2**) was

DOI: 10.1039/b311059a

**Table 1** The known iron(II)–thiolate complexes $[Fe^{II}(CO)_x(CN)_y(thiolate)]^{n-}$

| Compound | $y$ + thiolate | Reference |
|---|---|---|
| $[Fe(CO)_2(CN)(S_2C_6H_4\text{-}S,S)]^-$ | 1 + bidentate | 5*a* |
| **3** | 1 + bidentate | This work |
| **4** | 1 + tridentate | This work |
| $[Fe(CO)(CN)_2(S_2C_6H_4\text{-}S,S)]^{2-}$ | 2 + bidentate | 2 |
| $[Fe(CO)_2(CN)_2(S_2COR\text{-}S,S)]^-$ | 2 + bidentate | 5*b* |
| $[Fe(CO)_2(CN)_2(S_2CNR_2\text{-}S,S)]^-$ | 2 + bidentate | 5*b* |
| $[Fe(CO)_2(CN)_2(SPh)_2]^{2-}$ | 2 + 2(monodentate) | 2 |
| **1** | 2 + bidentate | This work |
| **6** | 3 + monodentate | This work |
| **7** | 3 + monodentate | This work |
| $[Fe(CO)(CN)_2(S_3)]^{2-}$ | 2 + tridentate | 4 |

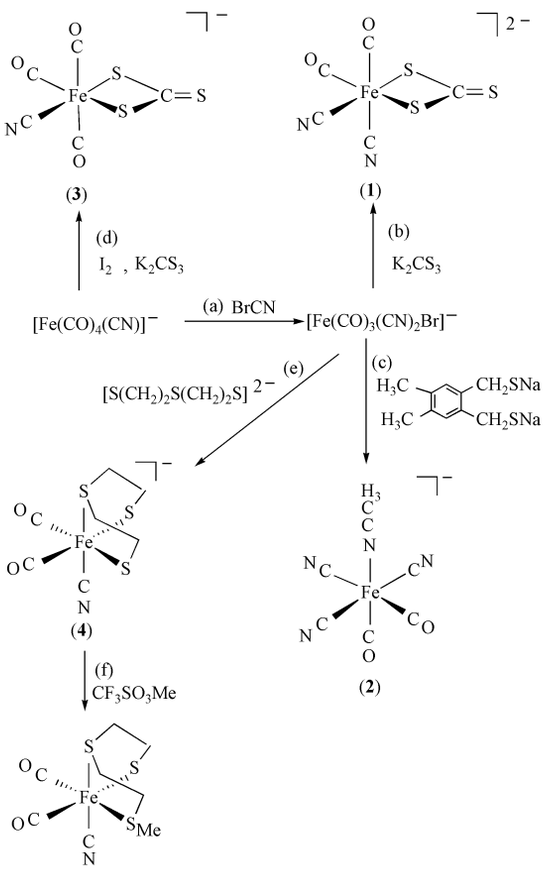


**Scheme 1**

obtained from reaction of $[Fe(CO)_3(CN)_2Br]^-$ and $Na_2[o\text{-}(SCH_2)_2C_6H_2\text{-}4,5\text{-}(CH_3)_2]$ (4,5-dimethyl-*o*-xylene-α,α′-dithiol) in $CH_3CN$ at room temperature after the mixture solution was precipitated by diethyl ether and extracted by thf (Scheme 1(c)). We proposed that the formation of complex **2** results from $[o\text{-}(SCH_2)_2C_6H_2\text{-}4,5\text{-}(CH_3)_2]^{2-}$ ligand dissociation of intermediate $[Fe(CO)_2(CN)_2(o\text{-}(SCH_2)_2C_6H_2\text{-}4,5\text{-}(CH_3)_2\text{-}S,S)]^{2-}$, followed by $CH_3CN$ coordination and cyanide $[CN]^-$ binding. The presumed intermediate $[Fe(CO)_2(CN)_2(o\text{-}(SCH_2)_2C_6H_2\text{-}4,5\text{-}(CH_3)_2\text{-}S,S)]^{2-}$ was not detected spectrally. The loss of the ligand $[o\text{-}(SCH_2)_2C_6H_2\text{-}4,5\text{-}(CH_3)_2]^{2-}$ from the $Fe^{II}$ center of the intermediate $[Fe(CO)_2(CN)_2(o\text{-}(SCH_2)_2C_6H_2\text{-}4,5\text{-}(CH_3)_2\text{-}S,S)]^{2-}$ may be due to the electron-rich character around the $Fe^{II}$ center (the lack of electron-delocalization around the $FeS_2C_4$ plane) and the more stable complex **2**. Obviously, the bidentate thiolates $[CS_3]^{2-}$ and $[o\text{-}(SCH_2)_2C_6H_2\text{-}4,5\text{-}(CH_3)_2]^{2-}$, render the $[Fe(CO)_2(CN)_2]$ motif in different electronic environments, induce differing stability to the $[Fe(CO)_2(CN)_2]$ unit (Table 1).

In order to evaluate the influence of $CN^-$ ligands on the stability and reactivity of the $Fe^{II}$–thiolate cyanocarbonyl complexes, a straightforward synthetic reaction of $[Fe(CO)_3(CN)I_2]^-$ (obtained from reaction of $[Fe(CO)_4(CN)]^-$ with 1 equiv of $I_2$) and $K_2CS_3$ in thf was conducted. The reaction resulted in the formation of the thermally unstable $[(CO)_3(CN)Fe(CS_3\text{-}S,S)]^-$ (**3**) under $N_2$ at ambient temperature (Scheme 1(d)). Following extended periods of stirring at room temperature, a thf solution of complex **3** converted into an insoluble solid. Presumably, the role of increments of $CN^-$ ligand coordinated to the Fe(II) center in complex **1**, compared to complex **3**, is to increase the electron density around the Fe(II) center as well as to stabilize the $Fe^{II}$ oxidation level. Interestingly, the reaction of the chelating $Na_2[S(CH_2)_2S(CH_2)_2S]$ ligand and $[Fe(CO)_3(CN)_2Br]^-$ yielded *cis*-$[Fe(CO)_2(CN)(S(CH_2)_2S(CH_2)_2S\text{-}S,S,S)]^-$ (**4**) in thf at ambient temperature (Scheme 1(e)). Formation of complex **4** can be interpreted as displacement of one cyanide ligand resulting from chelation of the tridentate $[S(CH_2)_2S(CH_2)_2S]^{2-}$ ligand. The extrusion of one σ-donor $CN^-$ ligand instead of CO from iron(II) center as a result of the reaction of $[Fe(CO)_3(CN)_2Br]^-$ and $Na_2[S(CH_2)_2S(CH_2)_2S]$ implicates the optimum electronic environment of the $[Fe^{II}(CO)_2]^{2+}$ fragment ligated by two thiolates, one thioether, and one cyanide (Table 1), as observed in the transformation of $[Fe(CN)_2(CO)_2(\mu\text{-}SEt)_2]_2^{2-}$ into the complex $[(CN)(CO)_2Fe(\mu\text{-}SEt)_3Fe(CO)_2(CN)]^-$ accompanied by extrusion of one σ-donor $CN^-$ ligand from each iron(II) center of the complex $[Fe(CN)_2(CO)_2(\mu\text{-}SEt)_2]_2^{2-}$ when ligated by the third bridging ethylthiolate.[12] Notably, both the electronic and steric reasons (chelation) are responsible for the formation of complexes **1**–**4**. Upon alkylation of complex **4** by $CF_3SO_3Me$ in thf at ambient temperature, the infrared spectrum shows the carbonyl/cyanide stretching bands 2046s, 1999s ($\nu_{CO}$), 2115w ($\nu_{CN}$) $cm^{-1}$ (thf), attributed to the thiolate-alkylated reaction to form the thermally unstable, neutral $[Fe(CO)_2(CN)(S(CH_2)_2S(CH_2)_2\text{-}SMe\text{-}S,S,S)]$ (Scheme 1(f)).

As shown in Scheme 2(a), when $[Me_3Si][CN]$ was reacted directly with $[Fe(CO)_3(CN)_2Br]^-$ in thf at room temperature, an air-stable hexacoordinate $Fe^{II}$ complex $[Fe(CO)_2(CN)_3Br]^{2-}$ (**5**) was isolated as a light yellow solid after recrystallization from $CH_3CN$–diethyl ether. The reaction solution led to the isolation of a mixture of *fac*-$[Fe(CO)_2(CN)_3Br]^{2-}$ and *mer*-$[Fe(CO)_2(CN)_3Br]^{2-}$ on addition of diethyl ether. The IR spectra (2039s, 1984br ($\nu_{CO}$), 2123vw, 2115w, 2105m ($\nu_{CN}$) $cm^{-1}$ ($CH_3CN$)) are consistent with a mixture of stereochemically fluxional isomers.

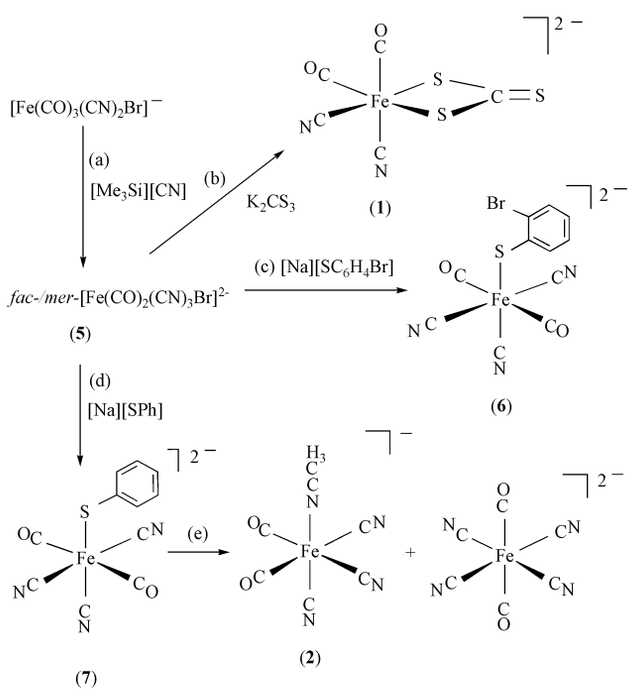


**Scheme 2**

Subsequent reactions of complex **5** with $K_2CS_3$ in $CH_2Cl_2$ produced the air and thermally stable complex **1** (Scheme 2(b)). Apparently, the dianionic $[CS_3]^{2-}$ ligand bound to the $Fe^{II}$ metal in a bidentate manner labilizes one cyanide ($[CN]^-$) ligand to yield complex **1**. The thermodynamic stability of complex **1** *vs.* **3**, **5** would then imply that the bidentate donor ligand $[CS_3]^{2-}$ substantially stabilizes the $[Fe^{II}(CO)_2(CN)_2]^0$, rather than the $[Fe^{II}(CO)_3(CN)]^+$ and $[Fe^{II}(CO)(CN)_3]^-$ motifs (Table 1).

We further examined the preparation of iron(II)–thiolate cyanocarbonyl species with the goal of investigating the influence of thiolate ligand(s) on the stability of the $[Fe^{II}(CO)_x(CN)_y(SR)_z]^{n-}$ species. The reaction of 2 equiv. of $Na[SC_6H_4Br]$ with a $CH_3CN$ solution of $[Fe(CO)_2(CN)_3Br]^{2-}$ afforded *mer*-$[Fe(CO)_2(CN)_3(m\text{-}SC_6H_4Br)]^{2-}$ (**6**), as determined by IR and X-ray diffraction (Scheme 2(c)). In a similar fashion, the ligand-displacement reaction was also displayed by reaction of complexes $[Fe(CO)_2(CN)_3Br]^{2-}$ and Na[SPh] (1 : 3 molar ratio) in $CH_3CN$ at 5 °C. IR spectroscopy of the $CH_3CN$ solution indicated the formation of a mixture of *mer*-$[Fe(CO)_2(CN)_3(SPh)]^{2-}$ (**7**) and traces of *trans*-$[Fe(CO)_2(CN)_4]^{2-}$ (Scheme 2(d) and (e)). The dominant product **7** was further purified by extraction into thf. Following extended periods of stirring at ambient temperature, a $CH_3CN$ solution of complex **7** converted into complex **2** and *trans*-$[Fe(CO)_2(CN)_4]^{2-}$ identified by IR and X-ray diffraction analysis (Scheme 2(e)). The thermodynamic instability of complex **7** may be attributed to the stronger σ-donor/π-donor properties of $[SPh]^-$ *vs.* $[m\text{-}SC_6H_4Br]^-$ ligands, although kinetic effects cannot be ruled out in the absence of rate studies. With this assignment, we may conclude that the less electron-donating monodentate thiolate ligand stabilizes the $[Fe^{II}(CO)_2(CN)_3]^-$ motif.

In order to corroborate this interpretation we treated a $CH_3CN$ solution of $[Fe(CO)_2(CN)_3Br]^{2-}$ with one equiv. of Na[SEt] at ambient temperature. The IR $\nu_{CO}/\nu_{CN}$ stretching frequencies are consistent with the formation of *trans*-$[Fe(CO)_2(CN)_4]^{2-}$, complex **2**, and $[(CN)(CO)_2Fe(\mu\text{-}SEt)_3Fe(CO)_2(CN)]^-$, presumably, resulting from transformation of the thermally unstable intermediate $[Fe(CO)_2(CN)_3(SEt)]^{2-}$ (**8**) (Scheme 3(a) and (b)). Thus, we can project an electron donor ability of the $[SEt]^-$ to $[Fe(CO)_2(CN)_3]^-$ unit to be more than that of the $[m\text{-}SC_6H_4Br]^-$ ligand, and this explains the relative instability of the intermediate **8**.

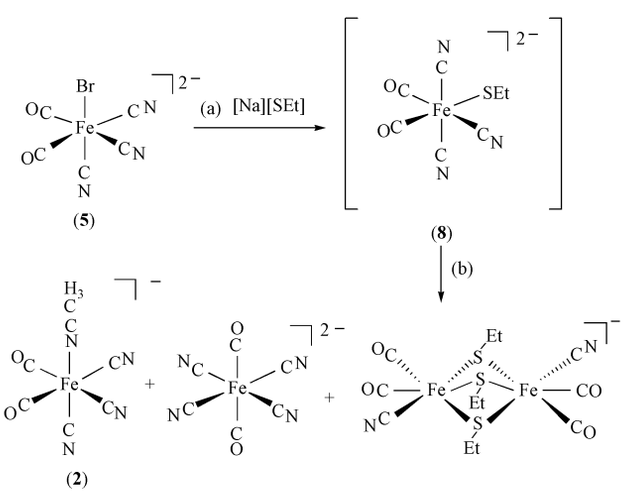


**Scheme 3**

Complex **1** contains particularly interesting functional groups, $[CS_3]^{2-}$ and $[CN]^-$, in which both the sulfur and nitrogen centers are potential sites of reactivity with electrophiles. Nucleophilic reaction of complex **1** with the hard alkylating reagent $CF_3SO_3Me$ in equimolar proportions in $CH_3CN$ at ambient temperature for 5 min yielded $[N(PPh_3)_2][Fe(CO)_2(CN)_2(CS_3Me\text{-}S,S)]$ (**9**) (Scheme 4(a)). The infrared spectra shows carbonyl/cyanide stretching bands (1997s, 2047s ($\nu_{CO}$), 2113w, 2122w ($\nu_{CN}$) $cm^{-1}$ ($CH_3CN$)), shifting from 1960s, 2016s ($\nu_{CO}$) 2102w, 2111w ($\nu_{CN}$) $cm^{-1}$ ($CH_3CN$), attributable to the presence of the chelating $[CS_3Me]^-$ ligand bound to the $[Fe(CO)_2(CN)_2]$ motif. $^1H$ NMR spectra ($\delta$ 2.499 (s) ppm ($CDCl_3$) ($[CS_3Me]^-$) become even more straightforward to confirm methylation of sulfur. There was no indication of nitrogen-site alkylation. This result implicates the reaction of complex **1** and electrophile occur at the more accessible, electron-rich sulfur site, although the thermodynamic product **9** does not necessarily reflect the initial, presumably, charge-controlled collision complex. Further addition of $CF_3SO_3Me$ to complex **9** in equimolar proportions in thf produces the charge-controlled collision product $[Fe(CO)_2(CN)(CNMe)(CS_3Me\text{-}S,S)]$ (**10**), characterized by the IR $\nu_{CNR}$ stretching frequency 2225 $cm^{-1}$ (2024s, 2069s ($\nu_{CO}$), 2128w, 2225m ($\nu_{CN}$) $cm^{-1}$ and $^1H$ NMR ($\delta$ 2.61 (s) (CNMe), 2.50 (s) ($CS_3Me\text{-}S,S$) ppm ($CDCl_3$)) (Scheme 4(b)).

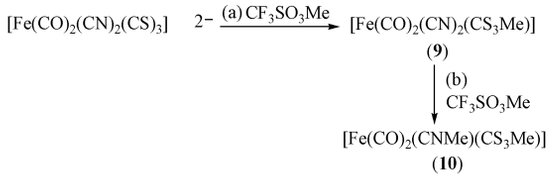


**Scheme 4**

## Structures

The molecular structures of complexes **1**–**7** are depicted in Figs. 1–7, respectively. Selected bond distances and angles are summarized in the captions of Figs. 1–7. The Fe–S bonds of average length 2.311(1) Å, Fe–C(O) bonds of average length 1.786(4) Å and Fe–C(N) bonds of average length 1.953(4) Å in complex **1** are within the range (2.2, 1.7 and 1.9 Å, respectively) observed in [NiFe] hydrogenases from *D. gigas*.[6] The two carbonyl groups of complex **2** are disposed in a *cis* arrangement and are *trans* to the $CN^-$ and $CH_3CN$ groups, respectively. The shorter Fe–C(5) bond (1.776(3) Å), as compared to 1.822(3) Å for the Fe–C(6) bond, is attributed to the π-back bonding character in complex **2**. The molecular structure of complex **3** anion is that of a distorted octahedron with S(1)–Fe(1)–S(2) bond angle of 74.04(2)°. The Fe–C(N) distance of 1.926(2) Å is comparable to that of the five-coordinate $[Fe(CO)_2(CN)(SNHC_6H_4\text{-}N,S)]^-$ (Fe–C(N) 1.926(6) Å).[5a]

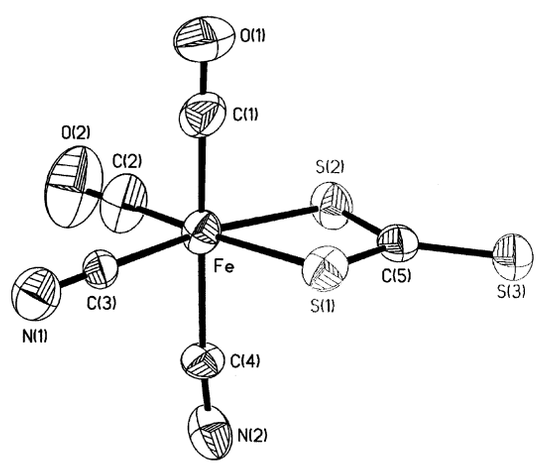


**Fig. 1** ORTEP drawing and labeling scheme of the $[Fe(CN)_2(CO)_2(CS_3\text{-}S,S)]^{2-}$ anion. Selected bond lengths (Å) and angles (°): Fe–C(2) 1.776(4), Fe–C(1) 1.796(4), Fe–C(3) 1.947(4), Fe–C(4) 1.960(3), Fe–S(2) 2.3109(10), Fe–S(1) 2.3119(11), S(1)–C(5) 1.725(4), S(2)–C(5) 1.719(4), S(3)–C(5) 1.669(4) Å; S(2)–Fe–S(1) 74.41(4)°.

The interesting feature of complex **4** is the asymmetry in the $Fe^{II}$–S bond lengths (Fe–S(2) 2.286(2) Å *vs.* Fe–S(1) 2.334(2) and Fe–S(3) 2.324(2) Å), which shows a difference of 0.043 Å

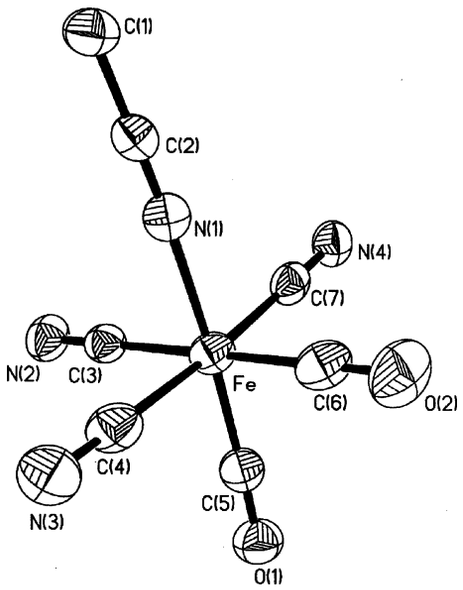


**Fig. 2** ORTEP drawing and labeling scheme of the $[Fe(CO)_2(CN)_3(NCCH_3)]^-$ anion. Selected bond lengths (Å): Fe–C(5) 1.776(3), Fe–C(6) 1.822(3), Fe–C(7) 1.927(3), Fe–C(3) 1.950(2), Fe–C(4) 1.943(3), Fe–N(1) 1.974(2) Å.

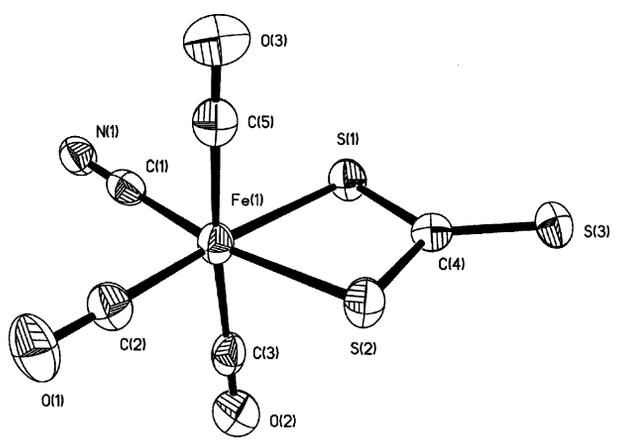


**Fig. 3** ORTEP drawing and labeling scheme of the $[Fe(CO)_3(CN)(CS_3\text{-}S,S)]^-$ anion. Selected bond lengths (Å) and angles (°): Fe(1)–C(2) 1.803(2), Fe(1)–C(5) 1.833(3), Fe(1)–C(3) 1.870(3), Fe(1)–C(1) 1.926(2), Fe(1)–S(1) 2.3315(6), Fe(1)–S(2) 2.3315(6), S(1)–C(4) 1.728(2), S(2)–C(4) 1.743(2), S(3)–C(4) 1.644(2) Å; S(1)–Fe(1)–S(2) 74.04(2)°.

between $Fe^{II}$–thioether and $Fe^{II}$–thiolate bonds. The two sulfur atoms of thiolates are disposed in a *cis* position and the positions *trans* to the sulfur atoms of thiolates are occupied by two CO ligands. This feature, as observed in complex **4**, can be attributed to the electronic influence of the $[S(CH_2)_2S(CH_2)_2S]^{2-}$ ligand. Because of disorder of $Br^-$ and $CN^-$ ligands in complex **5**, the exact Fe–C(N) bond lengths are poorly determined and the two carbonyl groups are disposed in a *cis* position. Owing to the disorder of $CN^-$ and $[SC_6H_4Br]^-$ in complex **6**, the exact Fe–S bond length is calculated as 2.424(5) Å, significantly longer than the Fe–S bond length of 2.375(1) Å in complex **7**.

## Conclusion

Studies on the mononuclear iron(II)–thiolate cyanocarbonyl complexes have led to the following results related to the structure, stability, and spectroscopic properties of the iron-site of bimetallic Ni–Fe active-site of [NiFe]-hydrogenases. As shown in Table 1, certain combinations of CO, $CN^-$ and thiolate ligands bound to the Fe(II) center play an important role in stabilizing the $[Fe^{II}(CO)_x(CN)_y(SR)_z]^{n-}$ species. The stabiliz-

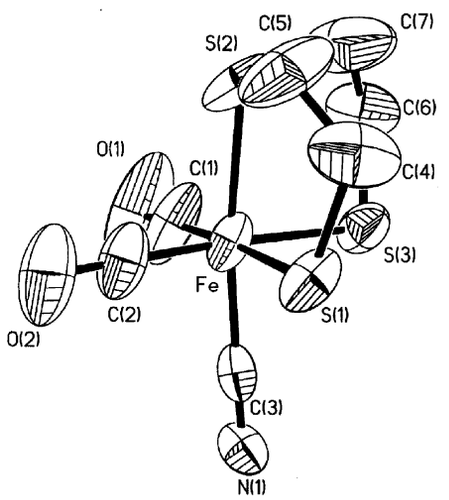


**Fig. 4** ORTEP drawing and labeling scheme of the $[Fe(CO)_2(CN)(S(CH_2)_2S(CH_2)_2S\text{-}S,S,S)]^-$ anion. Selected bond lengths (Å) and angles (°): Fe–C(2) 1.741(8), Fe–C(1) 1.778(8), Fe–C(3) 1.904(7), Fe–S(2) 2.286(2), Fe–S(3) 2.3236(19), Fe–S(1) 2.3338(17) Å; S(2)–Fe–S(3) 87.96(8), S(2)–Fe–S(1) 88.47(8), S(3)–Fe–S(1) 94.53(17)°.

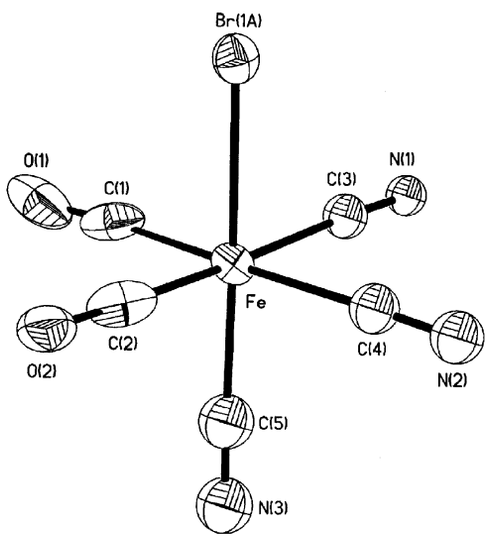


**Fig. 5** ORTEP drawing and labeling scheme of the $[Fe(CO)_2(CN)_3Br]^{2-}$ anion. Selected bond lengths (Å): Fe–C(2) 1.8114(19), Fe–C(1) 1.8162(19), Fe–C(5) 1.9659(19), Fe–C(3) 1.9874(18), Fe–C(4) 1.9883(19) Å.

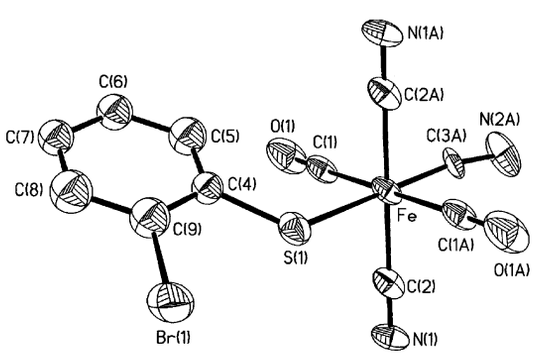


**Fig. 6** ORTEP drawing and labeling scheme of the $[Fe(CO)_2(CN)_3(o\text{-}SC_6H_4Br)]^{2-}$ anion. Selected bond lengths (Å): Fe–C(3) 1.850(9), Fe–C(2) 1.856(6), Fe–C(1) 1.900(5), Fe–S(1) 2.424(5) Å.

ation of various iron(II)–thiolate cyanocarbonyl complexes by the particular combinations of thiolate, cyanide and carbonyl ligation, (a) $[Fe^{II}(CO)_2(CN)_3]^-$ motif with monodentate thiolate ligand, (b) $[Fe^{II}(CO)_2(CN)_2]^0$ motif with bidentate thiolate ligands ($[S_2COR]^-$ and $[CS_3]^{2-}$) [5b] and (c) $[Fe^{II}(CO)_2(CN)]^+$ motif

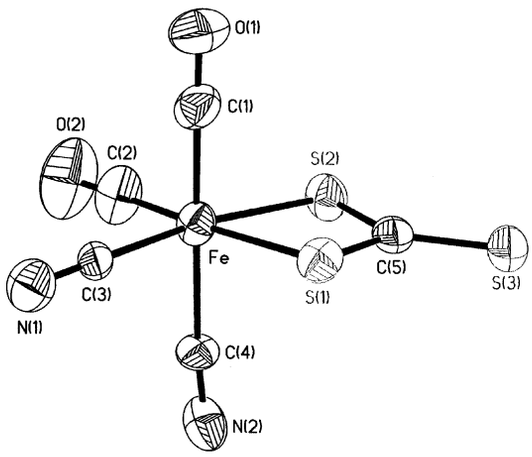


**Fig. 7** ORTEP drawing and labeling scheme of the $[Fe(CO)_2(CN)_3(SPh)]^{2-}$ anion. Selected bond lengths (Å): Fe(1)–C(5) 1.784(4), Fe(1)–C(1) 1.787(5), Fe(1)–C(2) 1.918(4), Fe(1)–C(3) 1.921(5), Fe(1)–C(4) 1.927(4), Fe(1)–S(1) 2.3751(12) Å.

with tridentate thiolate ligands, can be attributed to the optimum electronic environment of the Fe(II) center resulting from strong σ-donor $CN^-$, thiolate ligands as well as strong π-acceptor CO ligands. Notably, a certain total number of thiolate and cyanide ligands bound to the Fe(II) center stabilizes the binding of carbon monoxide to the Fe(II) metal, and this may point the way to understand the reasons for Nature's choice of combinations of these ligands in hydrogenases.

## Experimental

Manipulations, reactions, and transfers of samples were conducted under nitrogen according to standard Schlenk techniques or in a glove-box (argon gas). Solvents were distilled under nitrogen from appropriate drying agents (diethyl ether from $CaH_2$, acetonitrile from $CaH_2$–$P_2O_5$, methylene chloride from $P_2O_5$, hexane and tetrahydrofuran (thf) from sodium/benzophenone) and stored in dried, $N_2$-filled flasks over 4 Å molecular sieves. Nitrogen was purged through these solvents before use. Solvent was transferred to a reaction vessel *via* a stainless steel cannula under positive pressure of $N_2$. The reagents bis(triphenylphosphoranylidene)ammonium chloride ($[N(PPh_3)_2]Cl$), iron pentacarbonyl, 4,5-dimethyl-*o*-xylene-α,α′-dithiol, 2-bromothiophenol, 2-mercaptoethyl sulfide, sodium bis(trimethylsilyl) amide, ethanethiol, potassium trithiocarbomate monohydrate, and benzenethiol (Lancaster/Aldrich/Acros/Fluka) were used as received. Infrared spectra of the $\nu_{CO}$/$\nu_{CN}$ stretching frequencies were recorded on a Bio-Rad model FTS-185 and PerkinElmer model spectrum one B spectrophotometer with sealed solution cells (0.1 mm) and KBr windows. UV–vis spectra were recorded on a GBC Cintra 10e and a Hewlett Packard 71 spectrophotometers. Analyses of carbon, hydrogen and nitrogen were obtained with a CHN analyzer (Heraeus).

### Preparation of *cis*,*cis*-$[N(PPh_3)_2]_2[Fe(CO)_2(CN)_2(CS_3$-*S*,*S*$)]$ (*cis*,*cis*-$[N(PPh_3)_2][Et_4N][Fe(CO)_2(CN)_2(CS_3$-*S*,*S*$)]$) (1)

Into a 50 mL Schlenk flask were loaded the starting materials $[N(PPh_3)_2][Fe(CO)_3(CN)_2Br]$ (0.5 mmol, 0.4051 g),[5b] $K_2CS_3$ (0.5 mmol, 0.102 g), and $[N(PPh_3)_2]Cl$ (0.5 mmol, 0.287 g) (or $Et_4NCl$, 0.5 mmol, 0.084 g). A 10 mL portion of $CH_3CN$ was added to give a yellow–brown solution. The solution mixture was stirred at room temperature overnight. The resulting mixture was filtered and diethyl ether was added to precipitate the yellow–brown solid. 5 ml of thf was added to wash the yellow-brown solid. Recrystallization from $CH_3CN$–diethyl ether gave the yellow–brown solid *cis*,*cis*-$[N(PPh_3)_2]_2[Fe(CO)_2(CN)_2(CS_3$-*S*,*S*$)]$ (0.465 g, 68%) (or $[Et_4N][N(PPh_3)_2][Fe(CO)_2(CN)_2(CS_3$-*S*,*S*$)]$). Diffusion of diethyl ether into a $CH_3CN$ solution of complex **1** at −15 °C for 3 weeks yielded crystals suitable for X-ray crystallography. IR ($CH_3CN$): 1960s, 2016s ($\nu_{CO}$), 2102w, 2111w ($\nu_{CN}$) $cm^{-1}$. $^{13}C$ NMR ($CD_3CN$): δ 212.95 (d), 216.94 (d) ppm (CO). Absorption spectrum (thf) [$\lambda_{max}$/nm ($\varepsilon/M^{-1}$ $cm^{-1}$)]: 362 (6536) (Found: C, 68.77; H, 4.82; N, 4.20. Calc. for $C_{77}H_{60}N_4O_2P_4S_3Fe$: C, 68.54; H, 4.48; N, 4.15%).

### Reaction of $[N(PPh_3)_2][Fe(CO)_3(CN)_2Br]$ and $Na_2[o$-$(SCH_2)_2C_6H_2$-4,5-$(CH_3)_2$-*S*,*S*$]$

A $CH_3CN$ solution (10 mL) containing $[N(PPh_3)_2][Fe(CO)_3(CN)_2Br]$ (0.4051 g, 0.5 mmol) and $Na_2[o$-$(SCH_2)_2C_6H_2$-4,5-$(CH_3)_2]$ (0.099 g, 0.5 mmol, obtained from reaction of 4,5-dimethyl-*o*-xylene-α,α′-dithiol and Na[OMe])[5b] was stirred for 3 days at ambient temperature. The resulting mixture was filtered to remove the insoluble solid, and the yellow solution was then dried under vacuum. 5 ml of thf was added to the gray solid, the yellow solution was separated from the light yellow solid by filtration, and diethyl ether was slowly added to precipitate the yellow solid *mer*-$[N(PPh_3)_2][Fe(CO)_2(CN)_3(NCCH_3)]$ (**2**) (yield 0.190 g, 48%). Recrystallization by vapor diffusion of diethyl ether into a concentrated thf solution of complex **2** at −15 °C afforded yellow crystals. IR: 2009s, 2056s ($\nu_{CO}$), 2105w, 2117w ($\nu_{CN}$) $cm^{-1}$ (thf); 2068s, 2023s ($\nu_{CO}$), 2133w, 2127w, 2118w ($\nu_{CN}$) $cm^{-1}$ ($CH_3CN$). $^1H$ NMR ($CDCl_3$): δ 2.15 (s) ($NCCH_3$). Absorption spectrum (thf) [$\lambda_{max}$/nm ($\varepsilon/M^{-1}$ $cm^{-1}$)]: 340 (1109), 372 (757) (sh) (Found: C, 67.58; H, 4.15; N, 8.89. Calc. for $C_{43}H_{33}N_5O_2P_2Fe$: C, 67.11; H, 4.32; N, 9.10%).

### Preparation of *mer*-$[N(PPh_3)_2][Fe(CO)_3(CN)(CS_3$-*S*,*S*$)]$ (3)

A thf solution (10 mL) containing 0.366 g (0.5 mmol) of $[N(PPh_3)_2][Fe(CO)_4(CN)]$ and 0.127 g (0.5 mmol) of $I_2$ was stirred at room temperature for 2 h. The reaction was monitored immediately by IR. The spectrum (IR (thf): 2122w ($\nu_{CN}$), 2089m, 2047sh, 2039s ($\nu_{CO}$) $cm^{-1}$) was assigned to the formation of $[N(PPh_3)_2][Fe(CO)_3(CN)I_2]$. In the same flask, 0.5 mmol of $K_2CS_3$ (0.1022 g) was added, followed by stirring at room temperature for 2 h. The reaction mixture was filtered to remove KI, and hexane was added to precipitate the thermally unstable, red–brown solid *mer*-$[N(PPh_3)_2][Fe(CO)_3(CN)(CS_3$-*S*,*S*$)]$ (**3**) (0.334 g, 74%). To grow X-ray diffraction quality crystals, crystallization vials containing a concentrated thf solution of complex **3** were placed in a septum-sealed container surrounded by hexane. Upon standing at 0 °C for 3 weeks, red–brown crystals of **3** form. IR (thf): 2009s, 2033vs, 2076w, 2090vw ($\nu_{CO}$), 2123w ($\nu_{CN}$) $cm^{-1}$. Absorption spectrum (thf) [$\lambda_{max}$/nm ($\varepsilon/M^{-1}$ $cm^{-1}$)]: 412 (182).

### Preparation of *cis*-$[N(PPh_3)_2][Fe(CO)_2(CN)(S(CH_2)_2S(CH_2)_2$-S-*S*,*S*,*S*$)]$ (4)

Compound $[N(PPh_3)_2][Fe(CO)_3(CN)_2Br]$ (0.4051 g, 0.5 mmol)[5b] and $Na_2[S(CH_2)_2S(CH_2)_2S]$ (0.5 mmol, obtained from reaction of NaOMe and 2-mercaptoethyl sulfide $(HS(CH_2)_2S(CH_2)_2SH)$ in a 2 : 1 ratio in MeOH) were dissolved in 10 mL of thf and stirred for 5 h under nitrogen at 40 °C. The resulting mixture was filtered and diethyl ether–hexane was added to precipitate the orange solid *cis*-$[N(PPh_3)_2][Fe(CO)_2(CN)(S(CH_2)_2S(CH_2)_2S$-*S*,*S*,*S*$)]$ (yield 0.206 g, 47%). Diffusion of diethyl ether into thf solution of complex **4** at −15 °C for 3 weeks yielded yellow crystals suitable for X-ray crystallography. IR (thf): 1954s, 2009s ($\nu_{CO}$), 2101w ($\nu_{CN}$) $cm^{-1}$. $^1H$ NMR ($CDCl_3$): δ 3.08 (m) ($S(CH_2)_2S$). Absorption spectrum (thf) [$\lambda_{max}$/nm ($\varepsilon/M^{-1}$ $cm^{-1}$)]: 338 (1900) (Found: C, 61.97; H, 5.47; N, 3.80. Calc. for $C_{43}H_{38}N_2O_2P_2S_3Fe$: C, 62.31; H, 4.63; N, 3.38%). Upon alkylation of complex **4** by $CF_3SO_3Me$ in thf at ambient temperature, the infrared spectrum shows the carbonyl/cyanide stretching bands 2046s, 1999s ($\nu_{CO}$), 2115w ($\nu_{CN}$) $cm^{-1}$ (thf),

consistent with the formation of the thiolate-alkylated neutral $[Fe(CO)_2(CN)(S(CH_2)_2S(CH_2)_2SMeS,S,S)]$. $^1H$ NMR ($CDCl_3$): $\delta$ 1.23 (s) ($SCH_3$), 2.74 (m) ($S(CH_2)_2S$) ppm.

### Preparation of $[N(PPh_3)_2]_2[Fe(CO)_2(CN)_3Br]$ (5)

A solution containing 0.487 g (0.6 mmol) of $[N(PPh_3)_2][Fe(CO)_3(CN)_2Br]$ and 80 μL (0.6 mmol) of $Me_3SiCN$ in thf (8 mL) was added to 0.1722 g (0.3 mmol) of $[N(PPh_3)_2]Cl$ and the reaction mixture was stirred at ambient temperature for 2 days. A yellow solution accompanied by a light yellow solid was formed. The mother-liquor was removed under a positive pressure of $N_2$ and the yellow solid was redissolved in $CH_3CN$. The resulting mixture was filtered and diethyl ether was then added to precipitate a yellow solid, $[N(PPh_3)_2]_2[Fe(CO)_2(CN)_3Br]$ (yield 0.5388 g, 66%). Diffusion of diethyl ether into a $CH_3CN$ solution of complex **4** at −15 °C for 3 weeks yielded yellow crystals suitable for X-ray crystallography. IR ($CH_3CN$): 2039s, 1984br ($\nu_{CO}$), 2123vw, 2115w, 2105m ($\nu_{CN}$) $cm^{-1}$. Absorption spectrum ($CH_3CN$) [$\lambda_{max}$/nm ($\varepsilon$/$M^{-1}$ $cm^{-1}$)]: 324 (507), 383 (278) (Found: C, 68.35; H, 4.51; N, 4.87. Calc. for $C_{77}H_{60}BrN_5O_2P_4S_5Fe$: C, 68.66; H, 4.48; N, 5.20%).

### Preparation of *mer*-$[N(PPh_3)_2]_2[Fe(CO)_2(CN)_3(SC_6H_4Br)]$ (6)

A $CH_3CN$ solution (10 mL) containing complex **5** (0.539 g, 0.4 mmol) and $Na[SC_6H_4Br]$ (0.8 mmol, obtained from reaction of NaOMe and 2-bromothiophenol ($HSC_6H_4Br$) in a 1 : 1 ratio in MeOH) was stirred for 4 days at ambient temperature. The solution mixture was filtered to remove the insoluble solid and then diethyl ether was added to precipitate the yellow solid $[N(PPh_3)_2]_2[Fe(CO)_2(CN)_3(SC_6H_4Br)]$ (**6**) (yield 0.380 g, 65%). Recrystallization from a saturated $CH_3CN$ solution of complex **6** with diethyl ether diffusion at −10 °C gave orange–yellow crystals suitable for X-ray diffraction. IR ($CH_3CN$): 1978s, 2028s ($\nu_{CO}$), 2101w, 2112w, 2119w ($\nu_{CN}$) $cm^{-1}$. $^1H$ NMR ($CD_3CN$): $\delta$ 6.59–6.71 (m), 6.92–6.99 (m), 7.78–7.81 (m), 8.02–8.05 (m) ppm ($SC_6H_4Br$). Absorption spectrum ($CH_3CN$) [$\lambda_{max}$/nm ($\varepsilon$/$M^{-1}$ $cm^{-1}$)]: 418 (468) (Found: C, 69.19; H, 5.66; N, 5.58. Calc. for $C_{83}H_{64}N_5O_2P_4SBrFe$: C, 68.51; H, 4.43; N, 4.82%). The elemental analysis did not show good agreement with the calculated values because of the extreme thermal instability.

### Preparation of *mer*-$[N(PPh_3)_2]_2[Fe(CO)_2(CN)_3(SPh)]$ (7)

Into a 50-mL Schlenk flask were loaded the starting materials $[N(PPh_3)_2]_2[Fe(CO)_2(CN)_3Br]$ (0.539 g, 0.4 mmol), Na[SPh] (0.176 g, 1.2 mmol), and $[N(PPh_3)_2]Cl$ (0.459 g, 0.8 mmol). A 10 mL portion of $CH_3CN$ was added to give a yellow solution. The solution mixture was stirred at 5 °C for 4 days. The IR spectrum of the $CH_3CN$ solution shows peaks at 2118w, 2113w, 2100m, 2023s, 2000s, 1973s $cm^{-1}$, consistent with the formation of $[N(PPh_3)_2][Fe(CO)_2(CN)_3(SPh)]$ (**7**) and $[N(PPh_3)_2]_2[Fe(CN)_4(CO)_2]$. A 2 mL portion of diethyl ether was added and the resulting mixture was filtered to remove the insoluble solid *trans*-$[N(PPh_3)_2]_2[Fe(CN)_4(CO)_2]$. Diethyl ether (8 mL) was then added to precipitate the yellow solid. 5 ml of thf was added to extract the yellow product and the yellow solid *mer*-$[N(PPh_3)_2]_2[Fe(CO)_2(CN)_3(SPh)]$ (**7**) was isolated by washing with hexane (yield 0.076 g, 13.8%). Recrystallization from $CH_3CN$–diethyl ether gave yellow crystals suitable for X-ray diffraction. IR ($CH_3CN$): 1973s, 2023s ($\nu_{CO}$), 2100w, 2111vw, 2118vw ($\nu_{CN}$) $cm^{-1}$. $^1H$ NMR ($CD_3CN$): $\delta$ 7.51–7.69 (m), 7.31 (m) ppm ($SC_6H_5$). Absorption spectrum (thf) [$\lambda_{max}$/nm ($\varepsilon$/$M^{-1}$ $cm^{-1}$)]: 424 (229) (Found: C, 72.75; H, 4.84; N, 5.42. Calc. for $C_{83}H_{65}N_5O_2P_4SFe$: C, 72.44; H, 4.76; N, 5.09%). Following extended periods of stirring at ambient temperature, a $CH_3CN$ solution of complex **7** converted into complex **2** and *trans*-$[Fe(CO)_2(CN)_4]^{2-}$ identified by IR and X-ray diffraction analysis.

**Table 2** Crystallographic data for complexes **1**–**7**

| Complex | **1**·$CH_3CN$ | **2**·$H_2O$ | **3**·THF | **4**·1/2THF | **5** | **6** | **7** |
|---|---|---|---|---|---|---|---|
| Chemical formula | $C_{51}H_{53}FeN_5O_2P_2S_3$ | $C_{43}H_{37}FeN_5O_3P_2$ | $C_{45}H_{38}FeN_2O_4P_2S_3$ | $C_{48}H_{42}FeN_2O_{2.50}P_2S_3$ | $C_{77}H_{60}BrFeN_5O_2P_4$ | $C_{83}H_{64}BrFeN_5O_2P_4S$ | $C_{83}H_{65}FeN_5O_2P_4S$ |
| $M_r$ | 981.95 | 789.55 | 884.74 | 864.78 | 1346.94 | 1455.09 | 1376.19 |
| Crystal system | Monoclinic | Monoclinic | Triclinic | Monoclinic | Monoclinic | Monoclinic | Monoclinic |
| Space group | $P2_1/c$ | $P2_1/c$ | $P\bar{1}$ | $C2/c$ | $P2_1/c$ | $P2_1/c$ | $P2_1/c$ |
| $a$/Å | 16.5866(2) | 9.4354(4) | 9.8592(4) | 32.302(4) | 25.0227(2) | 10.9783(1) | 22.403(7) |
| $b$/Å | 19.4757(2) | 20.6670(8) | 14.9863(6) | 17.6622(19) | 13.0680(1) | 12.4250(2) | 14.834(4) |
| $c$/Å | 17.3778(2) | 20.3660(8) | 15.7414(6) | 15.0093(17) | 20.6298(2) | 28.5303(4) | 21.835(6) |
| $\alpha$/° | 90 | 90 | 115.8420(10) | 90 | 90 | 90 | 90 |
| $\beta$/° | 117.8531(5) | 90.4530(10) | 92.1350(10) | 91.137(2) | 107.4549(4) | 100.0536 (6) | 102.612(5) |
| $\gamma$/° | 90 | 90 | 90.4900(10) | 90 | 90 | 90 | 20 |
| $Z$ | 4 | 4 | 2 | 8 | 4 | 2 | 4 |
| $D_c$/g $cm^{-3}$ | 1.314 | 1.317 | 1.405 | 1.342 | 1.390 | 1.261 | 1.291 |
| $\mu$/$mm^{-1}$ | 0.539 | 0.506 | 0.633 | 0.614 | 1.008 | 0.878 | 0.385 |
| $T$/K | 150(1) | 150(2) | 293(2) | 150(2) | 120(1) | 150(1) | 293(2) |
| $R$ | 0.0574[a] | 0.0416[a] | 0.0382[a] | 0.0643[a] | 0.0627[a] | 0.0773[a] | 0.0506[a] |
| $R_w(F^2)$ | 0.1377[b] | 0.1178[b] | 0.1113[b] | 0.1641[b] | 0.1536[b] | 0.2275[b] | 0.1052[b] |
| GOF | 1.024 | 0.659 | 1.073 | 0.821 | 1.048 | 1.093 | 0.796 |

[a] $R = \Sigma||(F_o - F_c)|/\Sigma F_o$. [b] $R_w(F^2) = \{\Sigma w(F_o^2 - F_c^2)^2/\Sigma[w(F_o^2)^2]\}^{1/2}$.

### Reaction of $[N(PPh_3)_2]_2[Fe(CO)_2(CN)_3Br]$ and Na[SEt]

Into a 50-mL Schlenk flask were loaded the starting materials $[N(PPh_3)_2]_2[Fe(CO)_2(CN)_3Br]$ (0.539 g, 0.4 mmol) and Na[SEt] (0.038 g, 0.4 mmol). A 10 mL portion of $CH_3CN$ was added to give a brown solution. The solution mixture was stirred at room temperature for 4 days. The IR $\nu_{CO}/\nu_{CN}$ spectra shows the formation of complex **2** (2068s, 2023s, 2133w, 2127w, 2118w $cm^{-1}$), *trans*-$[Fe(CO)_2(CN)_4]^{2-}$ (2104m, 2000s $cm^{-1}$) and $[N(PPh_3)_2][(CO)_2(CN)Fe(\mu\text{-}SEt)_3Fe(CN)(CO)_2]$ (2106w, 2033w, 2020s, 1976s $cm^{-1}$).

### Crystallography

Crystallographic data of complexes **1**–**7** are summarized in Table 2. The crystals of **1**–**7** are chunky. Each crystal was mounted on a glass fiber. Diffraction measurements for complexes **1**, **2**, **4**, **6** were carried out at 150(2) K (293(2) K for complexes **3**, **7** and 120(1) K for complex **5**) on a Siemens SMART CCD diffractometer with graphite-monochromated Mo-Kα radiation ($\lambda$ = 0.71073 Å) and $\theta$ between 2.35 and 27.50° for complex **1**, between 1.40 and 27.53° for complex **2**, between 1.44 and 27.51° for complex **3**, between 1.26 and 27.55° for complex **4**, between 1.71 and 27.50° for complex **5**, between 1.79 and 27.50° for complex **6** and between 1.66 and 27.53° for complex **7**. Least-squares refinement of the positional and anisotropic thermal parameters for the contribution of all non-hydrogen atoms and fixed hydrogen atoms was based on $F^2$. Six atoms were refined isotropically for complex **5**. Due to disorder, the hydrogen atoms of the packing $H_2O$ and $C_4H_8O$ in complexes **2** and **4**, respectively, have not been refined. A SADABS [13] absorption correction was made. The SHELXTL [14] structure refinement program was employed.

CCDC reference numbers 217010–217016.

See http://www.rsc.org/suppdata/dt/b3/b311059a/ for crystallographic data in CIF or other electronic format.

## Acknowledgements

We gratefully acknowledge financial support from the National Science Council (Taiwan).

## References

1 (*a*) D. J. Darensbourg, J. H. Reibenspies, C.-H. Lai, W.-Z. Lee and M. Y. Darensbourg, *J. Am. Chem. Soc.*, 1997, **119**, 7903; (*b*) C. E. Coffey, *Inorg. Nucl. Chem.*, 1963, **25**, 179.

2 T. B. Rauchfuss, S. M. Contakes, S. C. N. Hsu, M. A. Reynolds and S. R. Wilson, *J. Am. Chem. Soc.*, 2001, **123**, 6933.

3 H.-F. Hsu, S. A. Koch, C. V. Popescu and E. Münck, *J. Am. Chem. Soc.*, 1997, **119**, 8371.

4 D. Sellmann, F. Geipel and F. W. Heinemann, *Chem. Eur. J.*, 2002, **8**, 958.

5 (*a*) W.-F. Liaw, N.-H. Lee, C.-H. Chen, C.-M. Lee, G.-H. Lee and S.-M. Peng, *J. Am. Chem. Soc.*, 2000, **122**, 488; (*b*) W.-F. Liaw, J.-H. Lee, H.-B. Gau, C.-H. Chen, S.-J. Jung, C.-H. Hung, W.-Y. Chen, C.-H. Hu and G.-H. Lee, *J. Am. Chem. Soc.*, 2002, **124**, 1680.

6 (*a*) A. Volbeda, M.-H. Charon, C. Piras, E. C. Hatchikian, M. Frey and J. C. Fontecilla-Camps, *Nature*, 1995, **373**, 580; (*b*) A. Volbeda, E. Garcin, C. Piras, A. L. de Lacey, V. M. Fernandez, E. C. Hatchikian, M. Frey and J. C. Fontecilla-Camps, *J. Am. Chem. Soc.*, 1996, **118**, 12989; (*c*) E. Garcin, X. Vernede, E. C. Hatchikian, A. Volbeda, M. Frey and J. C. Fontecilla-Camps, *Structure*, 1999, **7**, 557; (*d*) R. P. Happe, W. Roseboom, A. J. Pierik, S. P. Albracht and K. A. Bagley, *Nature*, 1997, **385**, 126.

7 (*a*) Y. Higuchi, H. Ogata, K. Miki, N. Yasuoka and T. Yagi, *Structure*, 1999, **7**, 549; (*b*) Y. Higuchi, T. Yagi and N. Yasuoka, *Structure*, 1997, **5**, 1671.

8 (*a*) A. L. de Lacey, E. C. Hatchikian, A. Volbeda, M. Frey, J. C. Fontecilla-Camps and V. M. Fernandez, *J. Am. Chem. Soc.*, 1997, **119**, 7181; (*b*) R. P. Happe, W. Roseboom and S. P. J. Albracht, *Eur. J. Biochem.*, 1999, **259**, 602; (*c*) H. Ogata, Y. Mizoguchi, N. Mizuno, K. Miki, S.-I. Adachi, N. Yasuoka, T. Yagi, O. Yamauchi, S. Hirota and Y. Higuchi, *J. Am. Chem. Soc.*, 2002, **124**, 11628–11635; (*d*) S. Foerster, M. Stein, M. Brecht, H. Ogata, Y. Higuchi and W. Lubitz, *J. Am. Chem. Soc.*, 2003, **125**, 83–93.

9 (*a*) Y. Nicolet, C. Piras, P. Legrand, E. C. Hatchikian and J. C. Fontecilla-Camps, *Structure*, 1999, **7**, 13; (*b*) Y. Nicolet, A. L. De Lacey, X. Vernede, V. M. Fernandez, E. C. Hatchikian and J. C. Fontecilla-Camps, *J. Am. Chem. Soc.*, 2001, **123**, 1596; (*c*) J. W. Peters, W. N. Lanzilotta, B. J. Lemon and L. C. Seefeldt, *Science*, 1998, **282**, 1853; (*d*) A. L. De Lacey, C. Stadler, C. Cavazza, E. C. Hatchikian and V. M. Fernandez, *J. Am. Chem. Soc.*, 2000, **122**, 11232; (*e*) C. V. Popescu and E. Münck, *J. Am. Chem. Soc.*, 1999, **121**, 7877.

10 (*a*) B. J. Lemon and J. W. Peters, *J. Am. Chem. Soc.*, 2000, **122**, 3793; (*b*) B. J. Lemon and J. W. Peters, *Biochemistry*, 1999, **38**, 12969; (*c*) B. Bennett, B. J. Lemon and J. W. Peters, *Biochemistry*, 2000, **39**, 7455.

11 L. Casalot and M. Rousset, *Trends Microbiol.*, 2001, **9**, 228.

12 W.-F. Liaw, W.-T. Tsai, H.-B. Gau, C.-M. Lee, S.-Y. Chou, W.-Y. Chen and G.-H. Lee, *Inorg. Chem.*, 2003, **42**, 2783.

13 G. M. Sheldrick, SADABS, Siemens Area Detector Absorption Correction Program, University of Göttingen, Germany, 1996.

14 G. M. Sheldrick, SHELXTL, Program for Crystal Structure Determination, Siemens Analytical X-ray Instruments Inc., Madison, WI, 1994.